Chinese Journal of Chemical Engineering 58 (2023) 146–154

Contents lists available at ScienceDirect

Chinese Journal of Chemical Engineering

journal homepage: www.elsevier.com/locate/CJChE

Full Length Article

Study on the epoxidation of olefins with H_2O_2 catalyzed by biquaternary ammonium phosphotungstic acid

Zijie Zhang, Qianyu Zha, Ying Liu, Zhibing Zhang, Jia Liu *, Zheng Zhou *

School of Chemistry and Chemical Engineering, Nanjing University, Nanjing 210093, China

ARTICLE INFO

Article history:
Received 31 May 2022
Received in revised form 7 November 2022
Accepted 8 November 2022
Available online 5 December 2022

Keywords:
Epoxidation of olefins
Phosphotungstic acid
Cyclohexene
Kinetic study

ABSTRACT

Selective epoxidation of olefins is an important field in chemical industry. In this work, we developed a new phosphotungstic acid catalyst $\{[(C_8H_{17})(CH_3)_2N]_2(CH_2)_3\}_{1.5}\{PO_4[WO(O_2)_2]_4\}$ with long carbon chain and biquaternary ammonium cation. Cyclohexene could be epoxidized to cyclohexene oxide in 96.3% conversion and 98.2% selectivity. The catalyst type, solvent type, catalyst loading, initial molar ratio, temperature, cycle performance and substrate extensibility were studied and optimized, the kinetic parameters about overall reaction and unit reaction were also calculated. Dynamic light scattering analysis was carried out to explain the different catalytic performance between catalysts with different carbon chain length. This novel catalyst and the corresponding dynamics and mechanism study could probably help the industrial application on the epoxidation of cyclohexene with H_2O_2.

1. Introduction

Selective epoxidation of olefins (high selectivity for epoxidation products) is an important field in chemical industry, since the epoxidation products are usually substantial intermediates for fine chemical production [1,2]. Cyclohexene oxide, one of the most essential chemical intermediate, is the raw material for the pesticides, resins, photosensitizers and many other fine chemicals [3,4].

However, the direct functionalization of numerous olefins to its epoxides remains a challenging task in catalytic domain. In the current industrial production, there are two main methods for the epoxidation of olefins. The halogenate-alcohol method is widely used for its simplicity and practicality, however, large amounts of wastewater with high content of chlorine is produced, causing serious environmental pollution. In the co-oxidation method, undesired by-products are produced in the meantime, resulting in low atomic availability. Therefore, there is an urgent need for novel methods to product epoxides, which are eco-friendly, atom economic and cost-efficient.

Using H_2O_2 [5–10] or molecular oxygen [11–16] as oxidant, the direct oxidation method has drawn lots of interest. Hydrogen peroxide is a green oxygen source, and the only by-product is water. Because of its mild catalytic activity, highly activity catalysts are needed for the epoxidation of alkenes. Various catalysts have been explored for the epoxidation of olefins, such as molecular sieve [17–19], metalloporphyrin complexes [20,21], MOFs [22,23] and heteropoly acid [24–26]. Particularly, phosphotungstic heteropoly acid can be prepared easily with high activity and selectivity for the epoxidation of olefins [4,27,28]. In 1983, Venturello *et al.* [29] used $PO^{3+}/WO_4^{2-}/O^+$ (5:2.5:1) as the catalytic system to catalyze the epoxidation of various olefins, with $CHCl_3$ as the solvent and H_2O_2 as the oxygen source. The conversion reached over 90% and the selectivity reached 80%. Although high yields have been achieved, the recovery of catalyst remained a major problem due to the liquid biphasic or homogeneous catalytic system.

On the other hand, in the current study, the kinetics mechanism of the epoxidation of olefins is rarely studied [30–33]. In 1995, Duncan *et al.* [34] deeply studied the catalytic mechanism of the $W^{VI}/P^{V}/H_2O_2/CHCl_3$/PTC (PTC = phase transfercatalyst) system, and confirmed that the active species $[PO_4[WO(O_2)_2]_4]^{3-}(PW_4)$ were formed in situ through the ^{31}P and ^{183}W spectrum. In 2009, Encho *et al.* [31] carried out kinetics study of the catalytic epoxidation of cyclohexene with *tert*-butyl hydroperoxide in the presence of molybdenum–squarate complex, and the kinetic parameters were obtained. In general, a systematized kinetic study hasn't been carried out yet in the field of epoxidation of cyclohexene with H_2O_2 catalyzed by biquaternary ammonium phosphotungstic acid.

* Corresponding authors.
E-mail addresses: liujia1@nju.edu.cn (J. Liu), zhouzheng@nju.edu.cn (Z. Zhou).

https://doi.org/10.1016/j.cjche.2022.11.009
1004-9541/

In this work, we developed a new type of phosphotungstic acid catalyst with long carbon chain and biquaternary ammonium cation (Fig. 1), and achieved a high conversion and selectivity over 95% in the epoxidation of cyclohexene with H_2O_2. The non-halogenated solvent CH_3CN was used to abate pollution, a good substrate universality and cycling performance was also confirmed in this catalytic system. The catalyst could be separated by simple filtering to be reused. We carried out the epoxidation reaction in various conditions and then conducted a kinetic study on both overall reaction and unit reaction. Besides, a significant effect of carbon chain length on catalytic performance was found, and colloidal theory was used to explain this phenomenon combined with DLS analysis.

2. Experimental

2.1. Catalyst preparation

The mixture of 100 mmol *N*,*N*,*N*′,*N*′-tetramethyl-1,3-propanediamine, 300 mmol 1-bromooctane and 150 ml isopropanol were stirred at 353 K for 18 h. Most of the isopropanol was removed through rotary evaporation. The resulting viscous liquid was transferred to the separation funnel and 50 ml of *n*-hexane was added each time. After considerable oscillation for a few minutes, we removed the upper cyclohexane solution which contained the unreacted substrate of *N*,*N*,*N*′,*N*′-tetramethyl-1,3-propanediamine and 1-bromooctane. After five times of the same operation, purified biquaternary ammonium bromide could be obtained, which was named as C_8-Br. Next, the C_8-Br was dried at 323 K for 12 h. Similarly, 1-bromooctane was substituted by bromides with different carbon chain lengths to prepared five other biquaternary ammonium bromides, named as C_4-Br, C_6-Br, C_{10}-Br, C_{12}-Br and C_{16}-Br respectively. While the mono-quaternary ammonium bromide, named as m-C_8-Br, was synthesized with *N*,*N*-dimethyl-*n*-octylamine as the substrate in a similar way.

Peroxo phosphotungstic acid compound $H_3[PO_4(WO(O_2)_2)_4]$ (H_3PW_4) was prepared according to the following method. 80.0 mmol Na_2WO_4 was dissolved in 100 ml water to obtain a clear solution. Next, 160 mmol of 36% (mass) hydrochloric acid was gradually added to obtain yellow-colored tungstic acid suspension. The suspension was stirred for 10 min and then added with 400 mol of 35% (mass) hydrogen peroxide. After the yellow-colored solid is completely dissolved, 20.0 mol of 85% (mass) phosphoric acid was added to prepare the peroxo phosphotungstic acid of $H_3[PO_4(WO(O_2)_2)_4]$.

The catalysts of biquaternary ammonium cation with different carbon chain lengths were prepared through ion exchange treatment of 20.0 mol $H_3[PO_4(WO(O_2)_2)_4]$ with excessive aqueous solution of biquaternary ammonium bromide (30.0 mmol) with different carbon chain lengths, and named as C_4-PW_4, C_6-PW_4, C_8-PW_4, C_{10}-PW_4, C_{12}-PW_4 and C_{16}-PW_4. m-C_8-Br was prepared in a similar way. Finally, the solution was removed by filtration, and the catalysts were washed with ethanol and deionized water consecutively for five times, then dried at 323 K for 8 h.

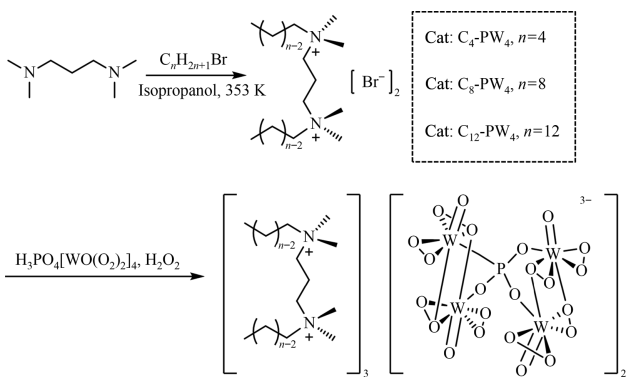

Fig. 1. The structure and synthesis pathway of the catalysts C_4-PW_4, C_8-PW_4 and C_{12}-PW_4.

2.2. Catalyst characterization

^{1}H nuclear magnetic resonance (^{1}H NMR) and ^{13}C nuclear magnetic resonance (^{13}C NMR) spectra were conducted on a BRUKER AVANCE III 400 NMR. Fourier transform infrared (FT-IR) spectra of samples were determined by Nicolet NEXUS 870 spectrometer using KBr as background atmospheric conditions. Raman spectra were conducted on LabRAM Aramis using a 633 nm laser. Thermogravimetric analysis (TGA) was performed on Netzche STA449F3 at a heating rate of 30 K·min^{-1} from 303 to 973 K under N_2 flowing. X-ray photoelectron spectroscopy (XPS) was performed on PHI5000 Versa Probe. Contact angle measurements were performed on Kruss DSA100.

2.3. Catalyst testing

The selective oxidation of cyclohexene was carried out in a four neck round flask (100 ml) equipped with a reflux condenser (water as cooling medium for the condensing to restrain the evaporation of cyclohexene and solvent).

Typically, 0.250 mmol catalyst, 10.0 mmol cyclohexene, 5.00 mmol H_2O_2 (35% (mass) solution in water) and 50 ml of CH_3CN were added into the flask. The mixture was heated in a water bath and stirred by a polytetrafluoroethylene stirring paddle, besides, a mercurial thermometer was immersed into the solution to make accurate temperature measurements. After the reaction, the catalyst was filtered off and washed with ethanol (15 ml × 4) and deionized water (15 ml × 4) consecutively for five times, then dried at 323 K for 8 h for reuse. The reactants and products were analyzed by Shimadzu GC 2014C with a capillary column WondaCAP-5 (30 m × 0.32 mm × 0.25 μm) and a flame ionization detector. The concentration of cyclohexene and products is determined through standard curve method, which is specified in Supplementary Material.

3. Results and Discussion

3.1. Catalyst characterization

The ^{1}H NMR and ^{13}C NMR spectra of the C_4-Br, C_6-Br, C_8-Br, C_{10}-Br, C_{12}-Br, C_{16}-Br and m-C_8-Br are shown in Figs. S2 and S3. In the ^{1}H NMR spectra, there are usually-seven proton peaks. The proton peaks whose $\delta > 3.0 \times 10^{-6}$ represent the α-H relative to N atom and the proton peaks whose $\delta > 1.6 \times 10^{-6}$ and $\delta < 2.2 \times 10^{-6}$ represent the β-H. Meanwhile, the proton peak which owns the minimal chemical shift indicates the protons of terminal methyl. Interestingly, it is found that the minimal chemical shift of proton peak reduces with the increase of carbon chain of biquaternary ammonium cation. This may be attributed to the steric hindrance of long carbon chains. In the ^{13}C NMR spectra, the carbon atom peaks whose $\delta > 50 \times 10^{-6}$ indicate the α-C relative to N atom. Taking both area and the chemical shift of the proton peaks and the carbon atom peaks into account, it is drawn the conclusion that the biquaternary ammonium cations of the catalysts have been prepared successfully.

According to the FT-IR spectra (Fig. 2, Fig. S4), the substrate C_8-Br is characterized by the following IR bands (in cm^{-1}): 2920 and 2850 (antisymmetric and symmetric vibration of C—H); 1420

(vibration of C—N). In the spectrum of the catalyst C_8-PW_4, new peaks (ν(P—O) at 1080 cm^{-1}, ν(W=O) at 950 cm^{-1}, ν(W—O—W) at 880 cm^{-1}, and $\nu(W(O)_2)$) at 550 cm^{-1}) are observed [35–37]. After treated with 35% H_2O_2, $H_3PW_{12}O_{40}$ shows similar infrared peaks, which are barely visible in the spectrum of the untreated $H_3PW_{12}O_{40}$. These results indicate that the PW_4 anion have replaced the bromine anion successfully. Above all, we have prepared the catalysts with the correct molecular structure.

In the Raman spectra (Fig. S5), the maximum peak of C_8-PW_4, which can be assigned to ν(W=O) [28], moves to a lower wavenumber compared with $H_3PW_{12}O_{40}$ from 1006 cm^{-1} to 875 cm^{-1}, which may attributed to the cation exchange of biquaternary ammonium.

In the XPS spectra (Fig. S6), the full survey spectra demonstrate the C 1s, O 1s, W 4p, W 4d, and W 4f signals at 285, 531, 429, 248 and 36 eV [4], respectively. The atomic ratio of W to P is about 4.06:1, and there are almost no bromine atoms, which supports a peroxo structure of $\{PO_4[WO(O_2)_2]_4\}^{3-}$ and its almost complete replacement of bromine anion.

As shown in Fig. S7, the TG curves of the C_8-Br and C_8-PW_4 show the high thermal stability of the catalyst C_8-PW_4 at temperature below 450 K. At temperature over 900 K, the mass of the C_8-Br is almost negligible. However, the catalyst C_8-PW_4 only losses nearly half of its mass owning to the high temperature resistance of tungsten element.

3.2. Catalyst screening

As shown in Table 1, we evaluated the catalyst performance of the C_4-PW_4, C_6-PW_4, C_8-PW_4, C_{10}-PW_4, C_{12}-PW_4, C_{16}-PW_4 with different carbon chain lengths and the m-C_8-PW_4, $H_3PW_{12}O_{40}$ and C_8-Br as control groups. In the series of catalysts of biquaternary ammonium cation with different chain lengths, C_8-PW_4 exhibited a highest 96.3% conversion and 98.2% selectivity of epoxy cyclohexene. In the control groups, we found C_8-PW_4 of biquaternary ammonium cation had greater advantage over m-C_8-PW_4 of mono-quaternary ammonium in catalytic activity. Meanwhile, $H_3PW_{12}O_{40}$ showed its poor catalytic activity with 10.3% conversion and 52.3% selectivity, and C_8-Br even showed no catalytic activity.

As a result, the introduction of biquaternary ammonium cation is beneficial to improve the catalytic activity of phosphotungstic heteropoly acid. C_8-PW_4, with the carbon chain length of 8, seems to be the most suitable catalyst for the epoxidation of cyclohexene with H_2O_2.

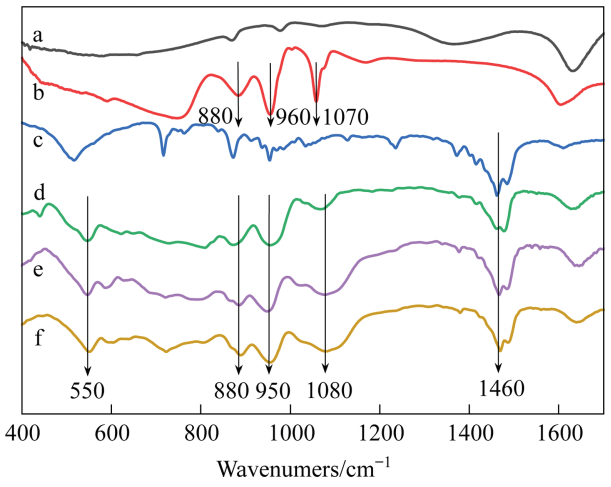

Fig. 2. FT-IR spectra of the catalysts and the substrates: (a) $H_3PW_{12}O_{40}$; (b) $H_3PW_{12}O_{40}$ treated with 35% H_2O_2; (c) C_8-Br; (d) C_4-PW_4; (e) C_8-PW_4; (f) C_{12}-PW_4.

From these results, we can see that the length of carbon chain plays an important role in the catalytic activity. As shown in Fig. S8, the C_4-PW_4 is completely soluble, while the C_8-PW_4 and C_{12}-PW_4 are insoluble. Moreover, the C_8-PW_4 is uniformly dispersed in the solution, but most of the C_{12}-PW_4 sticks to the wall of reactor. The C_8-PW_4 can be separated by filtration, moreover, it shows good dispersibility, which may help to improve its catalytic effect. Further, as shown in Table S7, we measured water contact angles of the catalysts. The contact angle will increase with the increase of carbon chain length of the catalysts. C_4-PW_4 shows strong hydrophilicity. It is difficult to determine its contact angle, the water-drop dropped on C_4-PW_4 surface will disappear within 30 s. The contact angle of C_8-PW_4 is 73.2°. It is close to 90°, which may explain its good dispersibility and catalytic activity. While the contact angle of C_{12}-PW_4 is 122.6°, this catalyst shows hydrophobicity and poor dispersion.

3.3. DLS analysis

We found emulsion formed during the reaction. Based on this, we carried out DLS analysis, which can obtain the particle size and distribution of droplet particles. We mixed the cyclohexene and hydrogen peroxide with the volume ratio of 1:5, then added the catalyst (0.025% (mol) of the cyclohexene). After ultrasonic processing for 3 min, we began the DLS analysis with 635 nm red laser. At this time, the emulsion type is oil in water (O/W), and we can get the size and distribution of the microdroplets of cyclohexene, which is shown in Fig. 3. And the primary data is shown in Fig. S9. The particle size distribution can be expressed by square deviation, which is calculated by Eq. (1).

$$s^2 = \sum_{i=1}^{n} (d_i - d_0)^2 x_i \quad (1)$$

where s^2 is the square deviation, d_0 is the mean diameter, d_i represents a certain diameter and x_i represents the corresponding proportion.

As shown in Fig. 3, we found the particle size of droplets decreased significantly, up to more than 50%, with the addition of the catalysts. We can attribute this phenomenon to the special structure of the biquaternary ammonium catalysts. For the catalysts, the long carbon chain part provides lipophilicity while the double quaternary ammonium cation part provides hydrophilicity. The amphiphilic catalysts act as surfactants to help the microdroplets of cyclohexene disperse into droplets with smaller particle size. Through the DLS between the three different types of catalysts, we found an inconspicuous distinction of the particle size, and the C_8-PW_4 group owned the minimum particle mean diameter at 401.4 nm. However, we found a clear difference of the particle distribution. The C_8-PW_4 group exhibited a minimum variance, which is only a quarter compared to other groups.

On the whole, the catalyst C_8-PW_4 helps the effective dispersion of cyclohexene droplets with the smallest size and the best uniformity. The catalytic reaction occurs at the droplet interface, which can explain the best catalytic effect, *i.e.* the fastest reaction rate and the highest selectivity, of the catalyst C_8-PW_4.

3.4. Effects of parameters

3.4.1. Effect of solvents

To investigate the influence of solvents, we chose eight kinds of representative solvents for experiments, and the result is shown in Table 2. As we can find, EtOAc exhibits excellent 95.7% conversion but only 1.3% selectivity of epoxy cyclohexene. The principal pro-

Table 1
Effects of various catalysts on the epoxidation of cyclohexene[①]

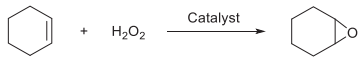

Catalyst	Conv.[②]/% (mol)	Sel./%		
		Epoxy–	–Diol	Others
C_4-PW_4	16.8	78.4	18.1	3.5
C_6-PW_4	65.7	90.5	8.2	1.3
C_8-PW_4	96.3	98.2	1.6	0.2
C_{10}-PW_4	90.2	98.0	1.8	0.2
C_{12}-PW_4	80.4	97.5	2.1	0.4
C_{16}-PW_4	77.8	97.8	1.7	0.5
m-C_8-PW_4	68.5	88.6	9.0	2.4
$H_3PW_{12}O_{40}$	10.3	52.3	39.8	7.9
C_8-Br	0	–	–	–

① Conditions: cyclohexene: 10.0 mmol, H_2O_2: 5.00 mmol (35% (mass) solution in water), catalyst: 0.0250 mmol, solvent: CH_3CN 5 ml, 400 r·min^{-1}, 308 K, 4 h.
② Conversion is related to H_2O_2.

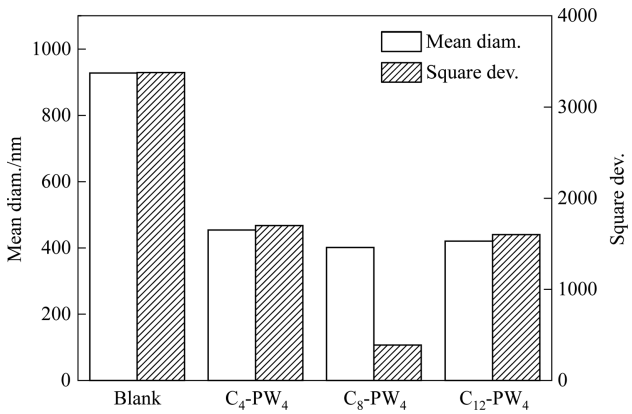

Fig. 3. DLS analysis of the size distribution and mean diameter. Initial volume ratio of H_2O_2 and cyclohexene, 5; catalyst, 0.025% (mol) of the cyclohexene.

duct is 2-ethoxycyclohexan-1-ol. While acetone shows considerable 98.8% selectivity of epoxy cyclohexene but relatively low conversion of 61.7%. And the product epoxy cyclohexene suffers from hydrolysis in the protic solvent MeOH and EtOH. However, it's worth mentioning that CH_3CN, chloroform and dichloromethane present both high conversion and selectivity. As a result, we choose CH_3CN as the most suitable solvent for its outstanding conversion of 96.3% and selectivity of 98.2%.

Generally, in polar aprotic solvents, C_8-PW_4 shows better catalytic performance both in conversion and selectivity. The addition of polar solvent may decrease the surface tension of water- cyclohexene interface, thus help the mixing of two phases. In polar protic solvents, C_8-PW_4 shows high conversion but low selectivity, because the epoxidation product is easily hydrolyzed in proton solvent. In weak polar solvent, C_8-PW_4 shows high selectivity, but the reaction rate is relatively slow.

3.4.2. Effect of catalyst loading

Experiments on the catalyst loading were carried out for 7.5 h at 308 K and an initial H_2O_2/cyclohexene molar ratio of 2, the result of which is shown in Fig. 4. The result shows that the reaction rate is increased when the catalyst loading rises from 0.0625 mmol to 0.250 mmol and then basically unchanged when the catalyst loading rises from 0.250 mmol to 0.313 mmol. Therefore, the catalyst loading should be maintained above 0.250 mmol to maximizing the use of catalyst activity.

With the increase of catalyst loading, the concentration of long carbon chain quaternary ammonium salt catalyst will be increased. Thus, the interfacial tension between oil and water will be reduced, which is conducive to the formation of smaller droplets and the increase of two-phase interface area, and the reaction rate will be improved. When the catalyst loading reaches 0.250 mol, the catalyst at the oil–water interface may have reached saturation, so the reaction rate is no longer significantly improved.

3.4.3. Effect of initial molar ratio of reactants

To investigate the influence of molar ratio, the initial ratio of cyclohexene and H_2O_2 was changed from 0.5:1 to 5:1, while other reaction conditions remained the same. The result is shown in Fig. 5. It is obviously shown that the conversion goes up from 48.9% to 95.3% as the cyclohexene/H_2O_2 ratio increases from 0.5:1 to 5:1. In the meantime, the reaction rate is increased when the cyclohexene/H_2O_2 ratio rises from 0.5:1 to 2:1 and then basically unchanged when the catalyst loading rises from 2:1 to 5:1. Thus, the initial cyclohexene/H_2O_2 molar ratio of 2 is more suitable under the reaction conditions.

3.4.4. Effect of reaction temperature

Reaction rate is closely related to the reaction temperature. Experiments on reaction temperature were conducted from 298 K to 318 K with other invariant conditions. As shown in Fig. 6, the reaction rate increases rapidly with increasing reaction temperature. In addition, the selectivity of epoxy cyclohexene shows a significant decrease when the temperature is higher than 308 K (Fig. S10). In consequence, we select 308 K as the most appropriate reaction temperature.

As the reaction temperature rises, the molecular motion becomes more active and the frequency of molecular collision increases, resulting faster reaction rate.

3.5. Kinetics study about reaction order and activation energy

In this section, we tend to calculate the orders of the reaction with respect to the concentrations of cyclohexene, H_2O_2 and catalyst. The expression of reaction rate can be expressed as

$$r = kC^m_{\text{cyclohexene}}C^n_{H_2O_2}C^l_{\text{catalyst}} \quad (2)$$

where k is the reaction rate constant, m, n and l are the reaction orders with respect to the concentrations of cyclohexene, H_2O_2 and catalyst respectively, and r is the reaction rate represented by the decrease of cyclohexene.

When we maintain the concentration of the two other substances unchanged, taking H_2O_2 and catalyst as example. Then we can get

Table 2
Effect of various solvents on the epoxidation of cyclohexene[①]

Solvent	Conv.[②]/% (mol)	Sel./%		
		Epoxy–	–Diol	Others
CH_3CN	96.3	98.2	1.6	0.2
Chloroform	80.4	90.7	8.7	0.6
Dichloromethane	76.2	93.2	6.3	0.5
MeOH	65.0	75.5	20.1	4.4
EtOH	73.5	81.0	16.2	2.8
EtOAc	95.7	1.3	8.5	90.2
1,4-dioxane	69.3	88.3	3.8	7.9
Acetone	61.7	98.8	0.8	0.4

① Conditions: Cyclohexene: 10.0 mmol, H_2O_2: 5.00 mmol (35% (mass) solution in water), Catalyst: C_8-PW_4 0.0250 mmol, Solvent: 5 ml; 400 r·min^{-1}; 308 K; 4 h.
② Conversion is related to H_2O_2.

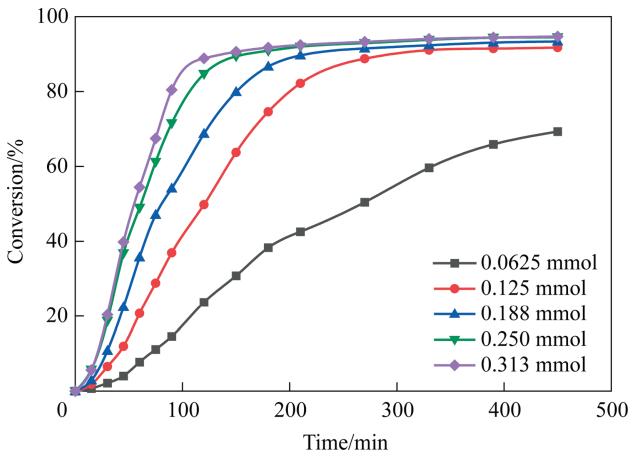

Fig. 4. Effects of catalyst loading on conversion relative to H_2O_2. Solvent, CH_3CN; initial molar ratio of cyclohexene/H_2O_2, 2; 308 K; 400 r·min^{-1}. (The amount of substance is based on the chemical formula $\{[(C_8H_{17})(CH_3)_2N]_2(CH_2)_3\}_{1.5}\{PO_4[WO(O_2)_2]_4\}$, which means the amount of the catalysts is equal to the amount of the active PW_4 part).

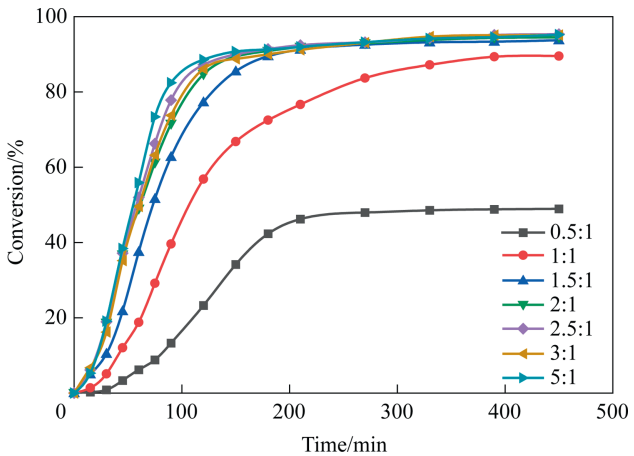

Fig. 5. Effects of initial molar ratio cyclohexene/H_2O_2 on conversion relative to H_2O_2. Solvent, CH_3CN; catalyst loading, 0.250 mmol; 308 K; 400 r·min^{-1}.

$$r = BC^{m}_{\text{cyclohexene}} \tag{3}$$

where B is a constant.

The order with respect to the concentrations of cyclohexene, m, can be obtained by fitting r and $C_{\text{cyclohexene}}$ to an exponential function. In the same way, we can calculate n and l. We conducted the experiments at the concentration of cyclohexene $C_{\text{cyclohexene}}$ = 0.315–0.788 mol·L^{-1}, the concentration of H_2O_2 $C_{H_2O_2}$ = 0.158–0.6

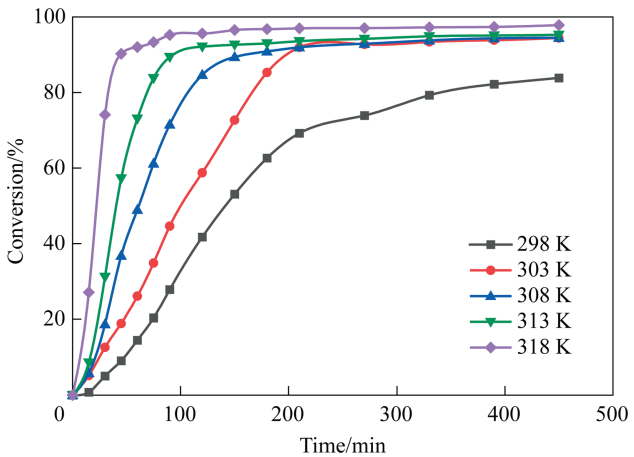

Fig. 6. Effects of reaction temperature on conversion relative to H_2O_2. Solvent, CH_3CN; catalyst loading, 0.250 mmol; initial molar ratio of cyclohexene/ H_2O_2, 2; 400 r·min^{-1}.

30 mol·L^{-1} and the concentration of catalyst C_{catalyst} = 0.00105–0.00420 mol·L^{-1}.

We find the kinetic curve is close to the S-shaped curve, hence we adopt logistic model to fit the curve. The logistic fitting function includes four mounting parameters and is shown in Eq. (4).

$$C = A_2 + \frac{A_1 - A_2}{1 + (t/t_0)^p} \tag{4}$$

The experimental data and the fitting curve are shown in Figs. S11–S13. Maximum slope of the fitting curve calculated by MATLAB is considered to be the reaction rate r, which is listed in Tables S1–S3. The r and C values are fitted according to Eq. (3), which is shown in Fig. 7, and the calculated reaction orders are listed in Table 3.

The expression of reaction rate is found to be

$$r = kC^{0.96}_{\text{cyclohexene}} C^{0.90}_{H_2O_2} C^{1.0}_{\text{catalyst}} \tag{5}$$

Approximatively, all the calculated reaction orders are 1.

Through the above experiments results, the relationship between cyclohexene concentration and reaction time under different temperature from 298 K to 318 K was obtained. We can get reaction rate r using similar method, and k can be calculated using Eq. (5) (Fig. S14, Table S4).

T dependence of k can be known from the Arrhenius equation

$$k = A_0 e^{-E_a/RT} \tag{6}$$

where A_0 represents the pre-exponential factor, and E_a is the activation energy.

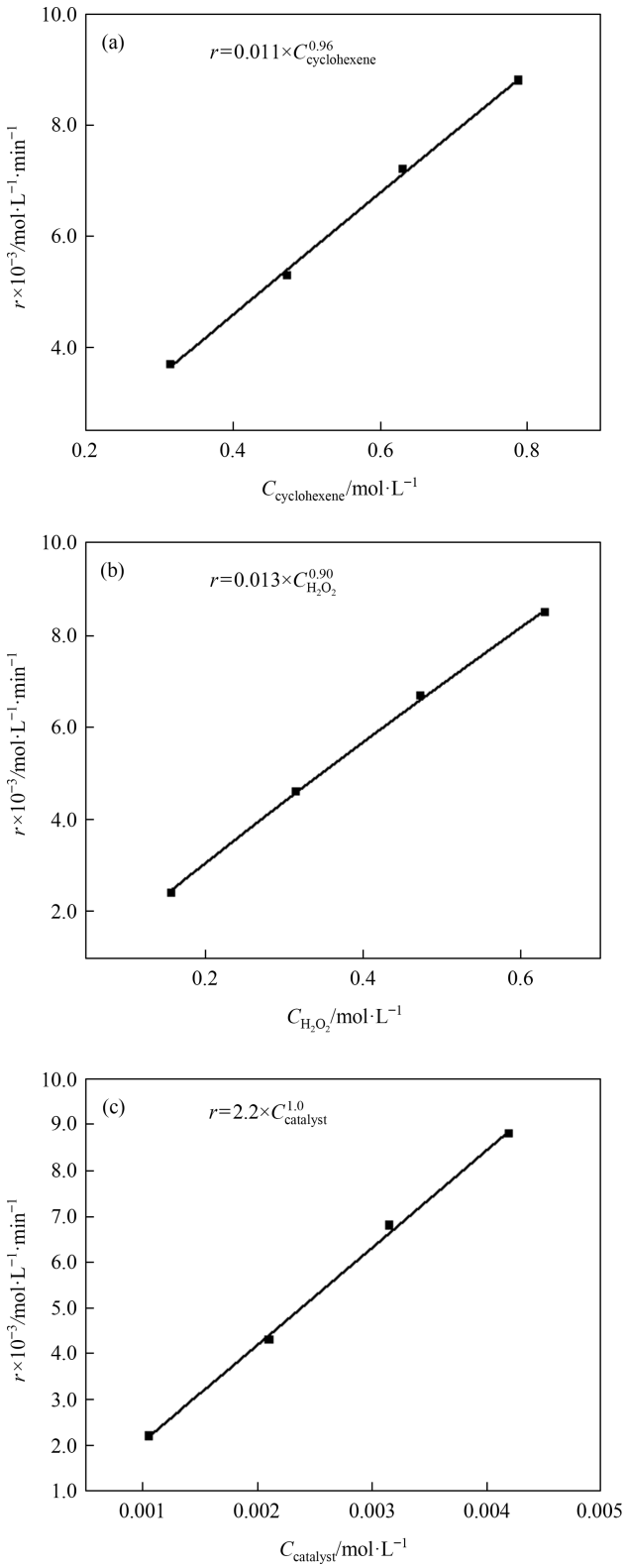

Fig. 7. C dependence of ln r: (a) r–$C_{cyclohexene}$; (b) r–$C_{H_2O_2}$; (c) r–$C_{catalyst}$.

Table 3
The orders of the reaction with respect to the concentrations of cyclohexene, H_2O_2 and catalyst: m, n, l

m	n	l
0.96 ± 0.03	0.89 ± 0.02	1.0 ± 0.04

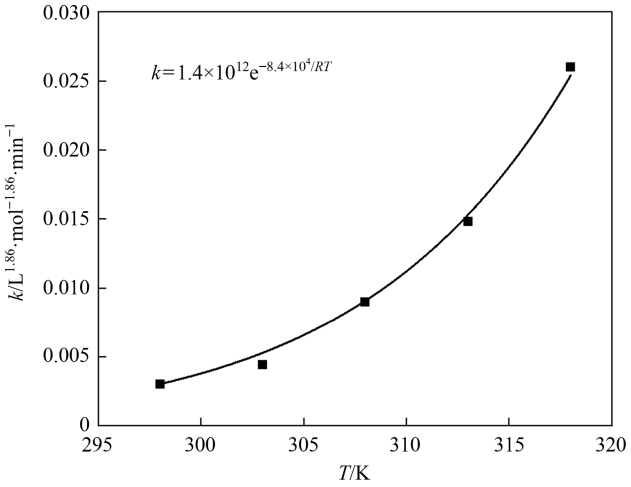

Fig. 8. T dependence of k.

Table 4
Pre-exponential factor A_0 and activation energy E_a

A_0/L$^{1.86}$·mol$^{-1.86}$·min^{-1}	E_a/kJ·mol^{-1}
$(1.4 \pm 0.3) \times 10^{12}$	84 ± 4

The activation energy E_a and the pre-exponential factor A_0 can be obtained by fitting k and T to Eq. (6), which is shown in Fig. 8. The calculation results of A_0 and E_a are listed in Table 4.

3.6. Kinetics study about rate constant of unit reaction

According to the previous literature, the epoxidation of cyclohexene with H_2O_2 reacts through intermediate of reactive oxygen species. To verify the generation of reactive oxygen species, the C_8-PW_4 was treated with 35% (mass) H_2O_2 and CH_3CN for 5 min, then dried at 323 K for 3 h. The corresponding FT-IR spectra is shown in Fig. S15.

In contrast with the untreated C_8-PW_4, we find a distinct new peak at 817 cm^{-1} in the spectrum of H_2O_2 treated C_8-PW_4, which represents vibration of O—O. The result indicates that the catalyst may form active oxygen species in the presence of hydrogen peroxide, then be involved in the oxidation of cyclohexene.

According to the conclusion above, we proposed the reaction mechanism through reactive intermediate formed from the phosphotungstic acid catalyst (Fig. 9).

The rate expressed as the decrease in the cyclohexene with time can be expressed as follows:

$$r = -\frac{\mathrm{d[cyclohexene]}}{\mathrm{d}t} = k_2[\mathrm{cyclohexene}][\mathrm{WO_2}] \quad (7)$$

where the total concentration of the catalyst is $[W]_T=[WO_2]+[WO]$.

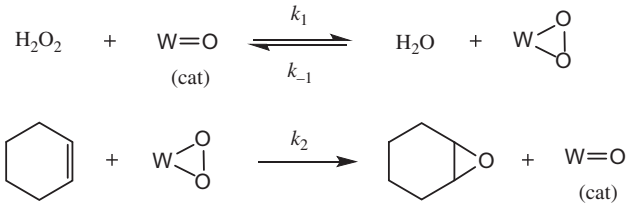

Fig. 9. Reaction mechanism through reactive intermediate.

When the concentration of H_2O_2 is much higher than that of cyclohexene and the expression $k_1[H_2O_2] + k_{-1} \gg k_2[\text{cyclohexene}]$ is satisfied, a rapid pre-equilibrium can be applied. Considering the mass balanced equation $[W]_T=[WO_2] + [WO]$ at the same time, we can derive the final rate equation without unknown variables.

$$r = -\frac{d[\text{cyclohexene}]}{dt} = \frac{k_1 k_2[\text{cat}][H_2O_2][\text{cyclohexene}]}{k_{-1} + k_1[H_2O_2] + k_2[\text{cyclohexene}]} \quad (8)$$

The experiments were carried out at 308 K and an initial H_2O_2/-cyclohexene molar ratio of 20, and then the experimental data was fitted to Eq. (8) using 1stOpt based on UGO. The resulting reaction rate constants k_1, k_{-1} and k_2 are listed in Table 5. The result shows that k_1 or k_{-1} is much larger than k_2, which proves the epoxidation of cyclohexene with the reactive intermediate is rate-determining step and the production of the reactive intermediate is a fast equilibrium process.

The experimental conversion and the calculated values from Eq. (8) are plotted in Fig. S16. The tiny fitting error verifies the mechanism of reactive intermediate we proposed.

Table 5
The reaction rate constants k_1, k_{-1} and k_2

k_1/L·mol^{-1}·min^{-1}	k_{-1}/L·mol^{-1}·min^{-1}	k_2/L·mol^{-1}·min^{-1}
55 ± 3	34 ± 2	7.4 ± 0.4

3.7. Cycling performance

The cycle experiments were conducted under the same conditions. The catalyst was filtered and purified after each cycle, then equivalent amount of reagents were added and reacted under the same conditions. The activity of the C_8-PW_4 still maintains a high level after five cycles (Table S5). We gain more than 95% conversion and selectivity during the cycle. As shown in Fig. S17, the IR spectrum of the recovered catalyst is consistent with that of the fresh catalyst. These results suggest that the catalyst can retain high recyclable stability and have a perfect prospect in industry application.

3.8. Substrate expansibility

The expansibility of the substrate was tested by using three kinds of olefins, the cycloolefins, chain olefins and aromatic alkenes. The results are listed in Table 6. We find the C_8-PW_4 show highest catalytic activity to the cycloolefins substrate. The epoxidation of chain olefins exhibits extremely high selectivity but slower reaction rate. In addition, the C_8-PW_4 shows poor catalytic activity to the styrene, considering that the π-π conjugation in styrene restrain the nucleophilic attack of reactive oxygen species. In conclusion, we verify our reaction system displays great substrate universality.

Table 6
Reactions of various olefins catalyzed by C_8-PW_4[①]

Entry	Substrate	Product	Time/h	Conversion[②]/% (mol)	Selectivity/%
1		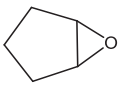	4 20	94.3 96.3	98.4 96.1
2		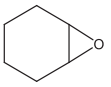	4 20	94.4 95.7	98.6 97.9
3		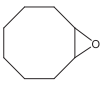	4 20	82.7 94.0	100 100
4	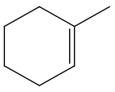	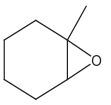	4 20	95.7 98.1	89.3[③] 96.3
5	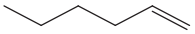	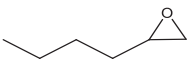	4 20	26.1 95.9	100 100
6	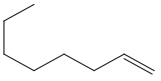	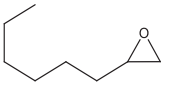	4 20	12.8 83.8	92.1 95.5
7	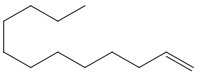	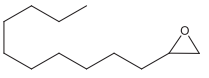	4 20	8.2 63.3	100 100
8	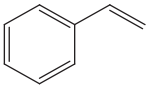	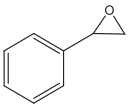	4 20	11.7 37.9	89.6[④] 86.6[④]
9	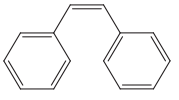	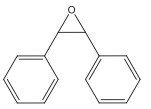	4 20	63.7 76.6	100 100

① Conditions: C_8-PW_4 (0.025 mmol), CH_3CN (5 ml), olefin (10 mmol), H_2O_2 (5 mmol, 35% (mass) solution in water), 400 r·min^{-1}, 308 K.
② Conversion is related to H_2O_2 %(mol).
③ The main by-product is α-enol.
④ The main by-product is benzaldehyde.

4. Conclusions

In this article, we prepared a new type of phosphotungstic acid catalyst with long carbon chain biquaternary ammonium cation. We screened out the catalyst C_8-PW_4 and found the influence of chain length to the catalyst activity. We found emulsion formed during the reaction and tried to explain the different catalytic effect between different catalysts through DLS analysis. Next, the optimum reaction conditions were obtained through several group of experiments. Kinetics study was conducted and related results such as activation energy and reaction order were obtained. By means of experimental characterization and dynamic simulation, a reaction mechanism through reactive intermediate was proposed and then confirmed, and corresponding reaction rate constants were acquired. At last, the excellent cycling performance and substrate universality of catalyst was verified. Moreover, our catalyst can be easily separated from solution by simple filtration, showing a promising future for industrial applications.

Data Availability

No data was used for the research described in the article.

Declaration of Competing Interest

The authors declare that they have no known competing financial interests or personal relationships that could have appeared to influence the work reported in this paper.

Acknowledgements

This research was supported by Natural Science Foundation of Jiangsu Province (BK20210185), National Natural Science Foundation of China (21776122).

Supplementary Material

Supplementary material to this article can be found online at https://doi.org/10.1016/j.cjche.2022.11.009.

Nomenclature

A_0	pre-exponential factor, $L^{1.86}\cdot mol^{-1.86}\cdot min^{-1}$
E_a	activation energy, $kJ\cdot mol^{-1}$
k	reaction rate constant, $L^{1.86}\cdot mol^{-1.86}\cdot min^{-1}$
k_1	positive reaction rate constant of the first elementary reaction, $L\cdot mol^{-1}\cdot min^{-1}$
k_2	reaction rate constant of the second elementary reaction, $L\cdot mol^{-1}\cdot min^{-1}$
k_{-1}	inverse reaction rate constant of the first elementary reaction, $L\cdot mol^{-1}\cdot min^{-1}$
l	reaction order of catalyst
m	reaction order of cyclohexene
n	reaction order of H_2O_2
r	reaction rate, $mol\cdot L^{-1}\cdot min^{-1}$
T	temperature, K
t	time, min

References

[1] A.S. Sharma, V.S. Sharma, H. Kaur, R.S. Varma, Supported heterogeneous nanocatalysts in sustainable, selective and eco-friendly epoxidation of olefins, *Green Chem.* 22 (18) (2020) 5902–5936.
[2] M. Mirzaee, B. Bahramian, J. Gholizadeh, A. Feizi, R. Gholami, Acetylacetonate complexes of vanadium and molybdenum supported on functionalized boehmite nano-particles for the catalytic epoxidation of alkenes, *Chem. Eng. J.* 308 (2017) 160–168.
[3] Y. You, C.Y. Luo, W.X. Zhu, Y.D. Zhang, Magnetic polymer microspheres based on phosphotungstic acid quaternary ammonium salt as an efficient heterogeneous catalyst for epoxidation of cyclohexene, *J. Iran. Chem. Soc.* 15 (7) (2018) 1535–1543.
[4] J. Liu, G.Q. Yang, Y. Liu, Z. Zhou, Z.B. Zhang, X.B. Hu, Selective oxidation of cyclohexene with H_2O_2 catalyzed by resin supported peroxo phosphotungstic acid under mild conditions, *Catal. Lett.* 151 (1) (2021) 147–152.
[5] D.T. Bregante, D.W. Flaherty, Periodic trends in olefin epoxidation over group IV and V framework-substituted zeolite catalysts: A kinetic and spectroscopic study, *J. Am. Chem. Soc.* 139 (20) (2017) 6888–6898.
[6] D.T. Bregante, N.E. Thornburg, J.M. Notestein, D.W. Flaherty, Consequences of confinement for alkene epoxidation with hydrogen peroxide on highly dispersed group 4 and 5 metal oxide catalysts, *ACS Catal.* 8 (4) (2018) 2995–3010.
[7] Y. Ding, W. Zhao, H. Hua, B.C. Ma, Π-$C_5H_5N(CH_2)_{15}CH_3]_3[PW_4O_{32}]/H_2O_2$/ethyl acetate/alkenes: A recyclable and environmentally benign alkenes epoxidation catalytic system, *Green Chem.* 10 (9) (2008) 910.
[8] J.M. Fraile, J.I. García, J.A. Mayoral, E. Vispe, Effect of the reaction conditions on the epoxidation of alkenes with hydrogen peroxide catalyzed by silica-supported titanium derivatives, *J. Catal.* 204 (1) (2001) 146–156.
[9] K. Hasan, N. Brown, C.M. Kozak, Iron-catalyzed epoxidation of olefins using hydrogen peroxide, *Green Chem.* 13 (5) (2011) 1230.
[10] W. Zhao, B.C. Ma, H. Hua, Y.S. Zhang, Y. Ding, Environmentally friendly and highly efficient alkenes epoxidation system consisting of [π-$C_5H_5N(CH_2)_{11}CH_3]_3PW_4O_{32}/H_2O_2$/ethyl acetate/olefin, *Catal. Commun.* 9 (14) (2008) 2455–2459.
[11] E.J. Marek, E.G.C. Conde, Effect of catalyst preparation and storage on chemical looping epoxidation of ethylene, *Chem. Eng. J.* 417 (2021) 127981.
[12] F.F. Li, J. Tang, Q.P. Ke, Y. Guo, M.N. Ha, C. Wan, Z.P. Lei, J. Gu, Q. Ling, V.N. Nguyen, W.C. Zhan, Investigation into enhanced catalytic performance for epoxidation of styrene over $LaSrCo_xFe_{2-x}O_6$ double perovskites: The role of singlet oxygen species promoted by the photothermal effect, *ACS Catal.* 11 (19) (2021) 11855–11866.
[13] K. Schröder, B. Join, A.J. Amali, K. Junge, X. Ribas, M. Costas, M. Beller, A biomimetic iron catalyst for the epoxidation of olefins with molecular oxygen at room temperature, *Angew. Chem. Int. Ed.* 50 (6) (2011) 1425–1429.
[14] Q.H. Tang, Q.H. Zhang, H.L. Wu, Y. Wang, Epoxidation of styrene with molecular oxygen catalyzed by cobalt(II)-containing molecular sieves, *J. Catal.* 230 (2) (2005) 384–397.
[15] Y.L. Wang, J. Deng, C. Zhang, W.F. Wu, Q.J. Xie, Y.C. Liu, Z.H. Fu, Epoxidation of cyclohexene with molecular oxygen by electrolysis combined with chemical catalysis, *J. Iran. Chem. Soc.* 11 (6) (2014) 1723–1729.
[16] C.R. Qi, J.Q. Hu, X. Zhou, Q. Wang, W.F. Xiong, L. Wang, R.K. Ye, G. Xiang, Epoxidation of alkenes with molecular oxygen as the oxidant in the presence of nano-Al_2O_3, *Synlett* 31 (18) (2020) 1789–1794.
[17] D. Lin, Q.D. Zhang, Z.X. Qin, Q. Li, X. Feng, Z.N. Song, Z.P. Cai, Y.B. Liu, X.B. Chen, D. Chen, S. Mintova, C.H. Yang, Reversing titanium oligomer formation towards high-efficiency and green synthesis of titanium-containing molecular sieves, *Angew. Chem. Int. Ed.* 60 (7) (2021) 3443–3448.
[18] Z.N. Song, X. Feng, N. Sheng, D. Lin, Y.C. Li, Y.B. Liu, X.B. Chen, X.G. Zhou, de Chen, C.H. Yang, Propene epoxidation with H_2 and O_2 on Au/TS-1 catalyst: Cost-effective synthesis of small-sized mesoporous TS-1 and its unique performance, *Catal. Today* 347 (2020) 102–109.
[19] J.G. Wang, T. Yokoi, J.N. Kondo, T. Tatsumi, Y.L. Zhao, Titanium(IV) in the organic-structure-directing-agent-free synthesis of hydrophobic and large-pore molecular sieves as redox catalysts, *ChemSusChem* 8 (15) (2015) 2476–2480.
[20] D.D. Aggrawal, D. Bhat, Halogenated tetraphenyl porphyrin; Iodosylbenzene an efficient catalytic system for olefin epoxidation, *J. Porphyrins Phthalocyanines* 19 (10) (2015) 1123–1129.
[21] L.D. Dias, R.M.B. Carrilho, C.A. Henriques, G. Piccirillo, A. Fernandes, L.M. Rossi, M. Filipa Ribeiro, M.J.F. Calvete, M.M. Pereira, A recyclable hybrid manganese (III) porphyrin magnetic catalyst for selective olefin epoxidation using molecular oxygen, *J. Porphyrins Phthalocyanines* 22 (4) (2018) 331–341.
[22] N. Candu, M. Tudorache, M. Florea, E. Ilyes, F. Vasiliu, I. Mercioniu, S.M. Coman, I. Haiduc, M. Andruh, V.I. Pârvulescu, Postsynthetic modification of a metal-organic framework (MOF) structure for enantioselective catalytic epoxidation, *ChemPlusChem* 78 (5) (2013) 443–450.
[23] H.F. Zhang, X.H. Lu, L. Yang, Y. Hu, M.Y. Yuan, C.L. Wang, Q.R. Liu, F.F. Yue, D. Zhou, Q.H. Xia, Efficient air epoxidation of cycloalkenes over bimetal-organic framework ZnCo-MOF materials, *Mol. Catal.* 499 (2021) 111300.
[24] L.I. Kuznetsova, N.I. Kuznetsova, Cyclohexane oxidation with an O_2–H_2 mixture in the presence of a two-component Pt/C–heteropoly acid catalyst and ionic liquids, *Kinetics Catal.* 58 (5) (2017) 522–532.
[25] M. Masteri-Farahani, M. Modarres, Wells-Dawson heteropoly acid immobilized inside the nanocages of SBA-16 with ship-in-a-bottle method: A new recoverable catalyst for the epoxidation of olefins, *J. Mol. Catal. A Chem.* 417 (2016) 81–88.
[26] C. Peng, X.H. Lu, X.T. Ma, Y. Shen, C.C. Wei, J. He, D. Zhou, Q.H. Xia, Highly efficient epoxidation of cyclohexene with aqueous H_2O_2 over powdered anion-resin supported solid catalysts, *J. Mol. Catal. A Chem.* 423 (2016) 393–399.
[27] W.J. Cai, Y. Zhou, R.L. Bao, B. Yue, H.Y. He, Catalytic epoxidation of cyclohexene over mesoporous-silica immobilized keggin-type tungstophosphoric acid, *Chin. J. Catal.* 34 (1) (2013) 193–199.

[28] J.H. Sun, X.X. Zhao, G.X. Sun, S. Zeb, Y. Cui, Q. You, Thermodynamic and kinetic study on the catalytic epoxidation of allyl chloride with H_2O_2 by new catalyst $[(C18H37)_2(CH_3)_2N]_3\{PO_4[W(O)(O_2)_2]_4\}$, *Chem. Eng. J.* 398 (2020) 125051.
[29] C. Venturello, E. Alneri, M. Ricci, A new, effective catalytic system for epoxidation of olefins by hydrogen peroxide under phase-transfer conditions, *J. Org. Chem.* 48 (21) (1983) 3831–3833.
[30] A.M. Al-Ajlouni, Ö. Sağlam, T. Diafla, F.E. Kühn, Kinetic studies on phenylphosphopolyperoxotungstates catalyzed epoxidation of olefins with hydrogen peroxide, *J. Mol. Catal. A Chem.* 287 (1–2) (2008) 159–164.
[31] E.H. Balbolov, S.V. Kotov, T.M. Kolev, M.G. Topuzova, Kinetics and mechanism of the catalytic epoxidation of cyclohexene with *tert*-butyl hydroperoxide in the presence of molybdenum–squarate complex, *React. Kinetics Catal. Lett.* 97 (1) (2009) 51–57.
[32] G.S. Owens, A. Durazo, M.M. Abu-Omar, Kinetics of MTO-catalyzed olefin epoxidation in ambient temperature ionic liquids: UV/Vis and 2H NMR study, *Chemistry* 8 (13) (2002) 3053–3059.
[33] D.A. Ruddy, T.D. Tilley, Kinetics and mechanism of olefin epoxidation with aqueous H_2O_2 and a highly selective surface-modified TaSBA15 heterogeneous catalyst, *J. Am. Chem. Soc.* 130 (33) (2008) 11088–11096.
[34] D.C. Duncan, R.C. Chambers, E. Hecht, C.L. Hill, Mechanism and dynamics in the $H_3[PW_{12}O_{40}]$-catalyzed selective epoxidation of terminal olefins by H_2O_2. Formation, reactivity, and stability of$\{PO_4[WO(O_2)_2]_4\}^{3-}$, *J. Am. Chem. Soc.* 117 (2) (1995) 681–691.
[35] H. Chen, W.L. Dai, R.H. Gao, Y. Cao, H.X. Li, K.N. Fan, New green catalytic manufacture of glutaric acid from the oxidation of cyclopentane-1, 2-diol with aqueous hydrogen peroxide, *Appl. Catal. A Gen.* 328 (2) (2007) 226–236.
[36] Y. Shen, X.H. Lu, C.C. Wei, X.T. Ma, C. Peng, J. He, D. Zhou, Q.H. Xia, Highly selective mono-epoxidation of dicyclopentadiene with aqueous H_2O_2 over heterogeneous peroxo-phosphotungstic catalysts, *Mol. Catal.* 433 (2017) 185–192.
[37] X. Zuwei, Z. Ning, S. Yu, L. Kunlan, Reaction-controlled phase-transfer catalysis for propylene epoxidation to propylene oxide, *Science* 292 (5519) (2001) 1139–1141.